

## RESEARCH ARTICLE

# Effects of bicyclol on hepatic sinusoidal obstruction syndrome induced by *Gynura segetum*

Jianzuo Yao<sup>1</sup> | Jingyi Wu<sup>2</sup> | Shu Jia<sup>2</sup> | Jingping Shao<sup>2</sup>  | Xie Zhang<sup>3</sup> | Zeping Xu<sup>3</sup>  | Hui Zhang<sup>4</sup> | Hong Li<sup>1</sup> | Xiaomin Yao<sup>2</sup> 

<sup>1</sup>Department of Hepatobiliary and Pancreatic Surgery, Li Huili Hospital Affiliated to Ningbo University, Ningbo, China

<sup>2</sup>Faculty of Pharmacy, Zhejiang Pharmaceutical University, Ningbo, China

<sup>3</sup>Department of Pharmacy, The affiliated hospital of Ningbo university, LiHuiLi Hospital, Ningbo, China

<sup>4</sup>The Second Affiliated Hospital and Yuying Children's Hospital of Wenzhou Medical University, Wenzhou Medical University, Wenzhou, China

## Correspondence

Hong Li, Department of Hepatobiliary and Pancreatic Surgery, Li Huili Hospital Affiliated to Ningbo University, Ningbo, China.

Email: [lancet2017@163.com](mailto:lancet2017@163.com)

Xiaomin Yao, Faculty of Pharmacy, Zhejiang Pharmaceutical University, Ningbo, China.

Email: [630088408@qq.com](mailto:630088408@qq.com)

## Funding information

Ningbo Digestive System Tumor Clinical Medicine Research Center, Grant/Award Number: 2019A21003; Ningbo Natural Science Foundation Project, Grant/Award Number: 202003N4336; Ningbo Public Welfare Science & Technology Major Project, Grant/Award Number: 2021S106; Ningbo Science and Technology Program Public Welfare Project, Grant/Award Number: 2019C50066, 2021S098 and 2021S144; Project of Zhejiang Medical and Health Platform Plan, Grant/Award Number: 2022KY1079; Zhejiang Provincial Medicine and Health Technology Project, Grant/Award Number: 2020RC106; Zhejiang Provincial Public Technology Research Projects, Grant/Award Number: LGF22H310003

## Abstract

**Background:** The intake of *Gynura segetum*, a traditional Chinese medicine, may be induce hepatic sinusoidal obstruction syndrome (HSOS). It has a high mortality rate based on the severity of the disease and the absence of therapeutic effectiveness. Therefore, the current study was designed to investigate the effects of bicyclol on HSOS induced by *Gynura segetum* and the potential molecular mechanisms.

**Methods:** *Gynura segetum* (30 g/kg) was administered for 4 weeks in the model group, while the bicyclol pretreatment group received bicyclol (200 mg/kg) administration. Serum alanine aminotransferase (ALT), aspartate aminotransferase (AST), cholesterol (CHO), triglyceride (TG), and liver histological assays were detected to assess HSOS. The gene expressions of cytochrome P450 (CYP450) isozymes were quantified by real-time PCR. Moreover, hepatocellular apoptosis was detected using the terminal deoxynucleotidyl transferase dUTP nick-end labeling (TUNEL) assay, then apoptosis and autophagy-related markers were determined using Western blot.

**Results:** As a result, bicyclol pretreatment is notably protected against *Gynura segetum*-induced HSOS, as observed by reducing serum ALT levels, inhibiting the reduction in CHO and TG levels, and alleviating the histopathological changes. Bicyclol pretreatment inhibited the changes in mRNA levels of CYP450 isozymes (including the increase in CYP2a5 and decrease in CYP2b10, 2c29, 2c37, 3a11, and 7b1). In addition, the upregulation of Bcl-2 and the downregulation of LC3-II/LC3-I proteins expression in HSOS were inhibited with bicyclol pretreatment.

**Conclusion:** Bicyclol exerted a protective effect against HSOS induced by *Gynura segetum*, which could be attributed to the regulated expressions of CYP450 isozymes and alleviated the downregulation of autophagy.

## KEYWORDS

autophagy, Bicyclol, cytochrome P450, *Gynura segetum*, HSOS

This is an open access article under the terms of the [Creative Commons Attribution-NonCommercial-NoDerivs](https://creativecommons.org/licenses/by-nc-nd/4.0/) License, which permits use and distribution in any medium, provided the original work is properly cited, the use is non-commercial and no modifications or adaptations are made.

© 2022 The Authors. *Journal of Clinical Laboratory Analysis* published by Wiley Periodicals LLC.

## 1 | INTRODUCTION

Hepatic sinusoidal obstruction syndrome (HSOS), also referred to as sinusoidal obstruction syndrome (SOS) or hepatic veno-occlusive disease (HVOD), is a non-thrombotic obstructive disease of the hepatic sinusoids characterized by the absence of thrombosis or other underlying hepatic venous disease.<sup>1,2</sup> The intake of special medicinal herbs, such as *Carpesii fructus*, *Lycopi herba*, is a primary etiology for HSOS due to the presence of the toxic substances known as pyrrolizidine alkaloids (PAs).<sup>3,4</sup> The major cause of HSOS in China is the ingestion of a PA-producing *Gynura segetum*, accounting for 50%–89% of reported HSOS cases.<sup>5</sup> However, the precise pathogenic mechanism of *Gynura segetum* causing HSOS is not clearly understood. Moreover, current therapeutic strategies for HSOS induced by PAs include cessation of exposure to PAs, symptomatic treatment, anticoagulant therapy, transjugular intrahepatic shunt (TIPS), and liver transplantation, which means that there is no definitive treatment for PA-induced HSOS.<sup>6</sup>

Bicyclol is an approved synthetic drug that has been widely used for the treatment of chronic viral hepatitis type B (HBV) and viral hepatitis type C (HCV) in China.<sup>7</sup> Previous studies have well documented that bicyclol exerts a protective effect against liver injuries in various experimental models with respect to several chemical and pharmaceutical toxins, ischemia–reperfusion and partial hepatectomy. This function is mediated by multiple mechanisms including antioxidant action, regulation of cytokine secretion, bidirectional regulation of expression of CYP450, inhibition of apoptosis and induction of cellular autophagy.<sup>8–13</sup> Our previous study reported that hepatocyte necrosis and autophagy occur in HSOS induced by *Gynura segetum*, while bicyclol has hepatoprotective and ameliorative effects on autophagy.<sup>14</sup> Taken together, bicyclol exerts hepatoprotective effects on various types of liver diseases via multipath signaling pathways, and may be used in the symptomatic treatment of HSOS induced by *Gynura segetum*; however, its effect related to HSOS or *Gynura segetum* has not been reported.

Therefore, the present study aimed to investigate the effects of bicyclol on HSOS induced by *Gynura segetum* and the potential molecular mechanisms.

## 2 | MATERIALS AND METHODS

This study was approved by the Experimental Animal Ethics Committee of Zhejiang Pharmaceutical College (Approval number: ZYLL202105019) and conducted in compliance with the Animal Research: Reporting of In Vivo Experiments (ARRIVE) guidelines.

### 2.1 | *Gynura segetum* extract and drug

The roots of 1000g *Gynura segetum* (acquired from Anhui Bozhou Pharmaceutical Co) were immersed in water for 2 h and boiled for 1.5 h, followed by filtration to collect filtrate A. The extracted roots

were supplemented with 3000ml of water, and the mixed decoction was boiled for 1.5 h as the above way, then filtered to obtain filtrate B. Finally, filtrates A and B were merged and boiled to reduce to a volume of 500ml that was refrigerated and reserved.<sup>15</sup> Bicyclol (No.200910) was procured from the Beijing Union Pharmaceutical Company.

### 2.2 | Animals and treatment

Male ICR mice (22–24g body weight, provided by the Zhejiang Academy of Medical Sciences) were used for the present study. A total of 30 mice were randomized into the control group, *Gynura segetum*-induced HSOS, and bicyclol-pretreated groups. The mice in the bicyclol-pretreated group were administered bicyclol (200mg/kg, suspended in 10% carboxymethyl cellulose) intragastrically twice daily for 4 weeks, while the other two groups were administered an equivalent volume of the vehicle of bicyclol as control. After 1 h, a 30g/kg concentrated decoction of *Gynura segetum* was administered by gavage in the *Gynura segetum*-induced HSOS group and bicyclol pretreated-groups, while an equivalent volume of distilled water was administered to the control group according to the same approach. At 4 weeks after administration, all mice were fasted for 12h, and then the liver tissues and blood samples (harvested through the eyeball) were immediately gathered. The liver tissues were freeze-clamped by liquid nitrogen and stored at –80°C to extract the mRNA and protein from the liver tissues. Approximately, 200mg of liver tissues were fixed in 10% formaldehyde prior to tissue freezing for histopathology. The plasma was collected from the blood samples by centrifugation at 3000g, 4°C for 10 min, and the content of alanine aminotransferase (ALT), aspartate aminotransferase (AST), cholesterol (CHO), and triglyceride (TG) was determined.

### 2.3 | Biochemistry analyses

Serum ALT, AST, CHO, and TG levels were, respectively, quantified using the corresponding assay kits (Ningbo Meikang Biological Co) on a biochemical analyzer (PUZS-300, Beijing Prolong New Technology Co), following the standard protocols.

### 2.4 | Histopathology

After mice were executed, liver tissues were fixed in 10% neutral formalin solution, then embedded in paraffin, sectioned at 5- $\mu$ m-thick sections, and stained with hematoxylin–eosin (H&E) and Masson for morphological observation. The pathology was assessed using a modified scoring system,<sup>16</sup> involving six parameters: sinusoidal hemorrhage, central venous subendothelial hemorrhage, hepatocyte-coagulative necrosis, central venous endothelial damage, central venous subendothelial fibrosis, and sinusoidal fibrosis. All sections were viewed under a light microscope (Olympus), and

the images were captured at  $\times 100$  magnification. Scoring system of pathology is evaluated by a pathologist based on the number of corresponding cells or pathological structures in the field of view at the same magnification of the microscope. Liver fibrosis was evaluated by Masson's staining and quantified by ImageJ software.

## 2.5 | Real-time polymerase chain reaction (RT-PCR) assay

Total RNA was extracted from mice liver samples using TRIzol reagent (Vazyme Biotech Co., Ltd). The cDNA was produced using a total of 1  $\mu$ g of RNA with the HiScript III All-in-one RT Reagent kit (Vazyme Biotech Co., Ltd). Finally, the gene expression was examined using the ChamQ SYBR Mixture real-time detection system. The reaction mixture in a volume of 20  $\mu$ l as follows: cDNA (2  $\mu$ l), ChamQ SYBR Mixture (10  $\mu$ l, Vazyme Biotech), and 0.5  $\mu$ l of each primer (10 pM). The amplification conditions were as follows: 95°C (30s), followed by 40 cycles of 95°C (10 s) and 60°C (30s). The primers are listed in Table 1.

## 2.6 | TUNEL assay

Terminal deoxynucleotidyl transferase (TdT)-mediated dUTP nick end labeling (TUNEL) assay was utilized to detect liver tissues with a situ cell apoptosis detection kit (Wuhan Boster Biological Engineering Co. Wuhan). The paraffin-embedded tissue sections were pretreated with proteinase K for 15 min and incubated with TdT and DIG-d-UTP labeling buffer at 37°C in a humidified chamber for 2 h. Next, the sections were flushed with a Tris-buffered saline (TBS) buffer for 2 min and incubated in a blocking buffer at 37°C for 30 min. Then, the sections were incubated in biotinylated

anti-digoxin antibodies (1:100 dilution) at 37°C for 40 min and rinsed with TBS buffer three times for 2 min. Subsequently, streptavidin-fluorescein (FITC) was used to stain the sections that were then rinsed with TBS buffer for 5 min, five times. Ultimately, the sections were placed in an antifading solution and examined under a fluorescence microscope. The positive cells with green color were quantified by ImageJ software.

## 2.7 | Protein extraction and Western blot assay

Liver tissues of mice in every group were lysed with radioimmunoprecipitation (RIPA) buffer (Beyotime Institute of Biotechnology). The supernatants were then collected by centrifugation at 13,000 rpm for 15 min at 4°C. Next, protein concentrations were detected with the BCA protein assay kit (TianGen Biotech Co). A western blot was conducted using total protein (10–50  $\mu$ g). Primary antibodies including anti-Caspase-3, B cell lymphoma/leukemia (Bcl)-2 (Bcl-2), LC3, autophagy-related 12 (Atg12), and  $\beta$ -actin were detected, and corresponding horseradish peroxidase-conjugated anti-rabbit or anti-goat were employed as secondary antibodies (all antibodies were from ProteinTech Group, Inc). Ultimately, the specific protein bands were visualized using an ECL Western Blot Detection System (LAS 400 Mini, General Electric Company, Boston).

## 2.8 | Statistical analysis

All data were expressed as mean  $\pm$  standard deviation (SD) and analyzed using one-way analysis of variance (ANOVA) by Graph Pad Prism 9.0 software. The differences between means were analyzed by Student–Newman–Keuls (SNK) test for multiple comparisons. Statistical significance was set at  $p < 0.05$ .

TABLE 1 Polymerase chain reaction primer sets in real-time PCR.

Gene	Primer sequences	GenBank™ accession no.
CYP2A5	Forward TGTAGTCAGCACCAAGTTC Reverse CTCCTTCTCATCCGAATG	NM_007812
CYP2B10	Forward GGCACCTCCAATAGGTATAAGA Reverse CAGTCATCCACGAGATTCA	NM_009999
CYP2C29	Forward GCTTCCTTCACTGCTTCA Reverse GCCAATCCTTACCAACT	NM_007815
CYP2C37	Forward CTTCACTGCCTCATATCCAT Reverse GACATCTGCCAATCCTTCA	NM_010001
CYP3A11	Forward CTCTCAAGTCTATTAGCAATGG Reverse AGATGGAATACCTGGATATGG	NM_007818
CYP7B1	Forward TCTGTGTTCCAATCTGTGAT Reverse GCTTACTGATGACGACCTT	NM_007825

Abbreviations: CYP2A5, cytochrome P450, family 2, subfamily a, polypeptide 5; CYP2B10, cytochrome P450, family 2, subfamily b, polypeptide 10; CYP2C29, cytochrome P450, family 2, subfamily c, polypeptide 29; CYP2C37, cytochrome P450, family 2, subfamily c, polypeptide 37; CYP3A11, cytochrome P450, family 3, subfamily a, polypeptide 11; CYP7B1, cytochrome P450, family 7, subfamily b, polypeptide 1.

### 3 | RESULTS

#### 3.1 | Effect of bicyclol on the changes of serum biochemical indicators in HSOS mice

As illustrated in Figure 1, serum ALT and AST levels in the HSOS group were increased to 8.6- and 2.3-fold of the control group, respectively. After bicyclol pretreatment, the level of serum ALT in the HSOS group declined remarkably, while the decrease in AST level was not statistically significant. In addition, compared to the control group, serum CHO and TG levels in the HSOS group were decreased to 64.7% and 29.0%, and bicyclol pretreatment can significantly ameliorate the reduction in serum CHO and TG levels (Figure 1C,D).

#### 3.2 | Effects of bicyclol on the changes in liver histopathology in HSOS mice

To directly evaluate the effect of bicyclol on HSOS, H&E, and Masson's staining of the liver tissues were performed. As shown in Figures 2,3, compared to the control group, the liver histopathological changes in the *Gynura segetum*-induced HSOS group show central venous endothelial damage and hemorrhage, severe sinusoidal congestion and space narrowing, coagulative necrosis of hepatocytes, inflammatory cell accumulation and fibrosis in portal areas, some hepatocyte nucleus pyknosis, fatty degeneration of hepatocytes, and liver lobule structure destruction. The pretreatment with bicyclol relieved the above histopathological changes induced by *Gynura segetum*. The pathological evaluation of every group is shown in Table 2.

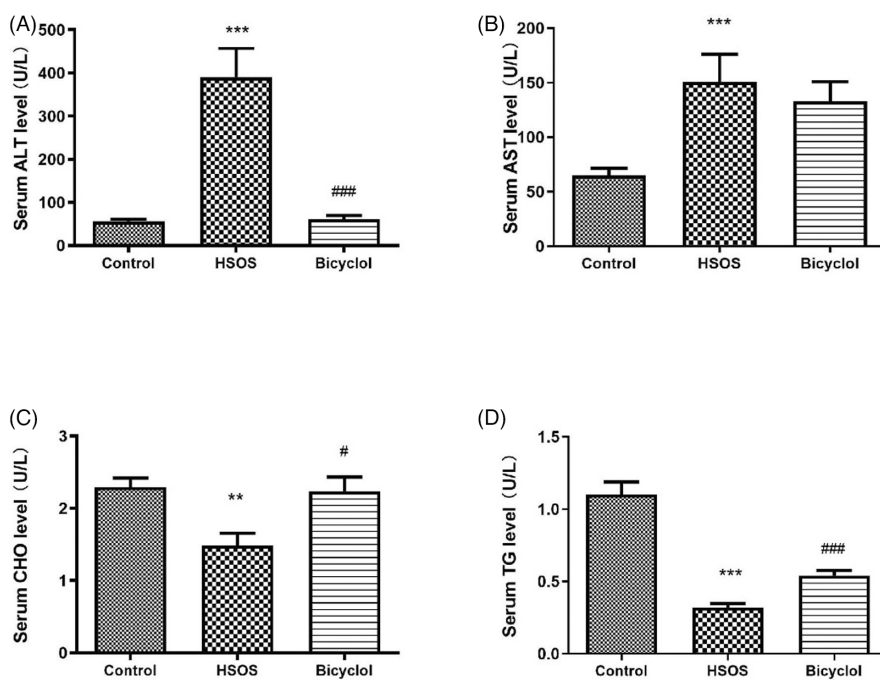


**FIGURE 1** Effect of bicyclol on the increase in serum transaminases and serum lipids in HSOS mice. Samples of blood were collected at 4 weeks after *Gynura segetum* administration: (A) serum ALT; (B) serum AST; (C) serum CHO; (D) serum TG. \*\* $p < 0.01$  versus control group, \*\*\* $p < 0.001$  versus control group, # $p < 0.05$  versus HSOS group, ### $p < 0.001$  versus HSOS group.

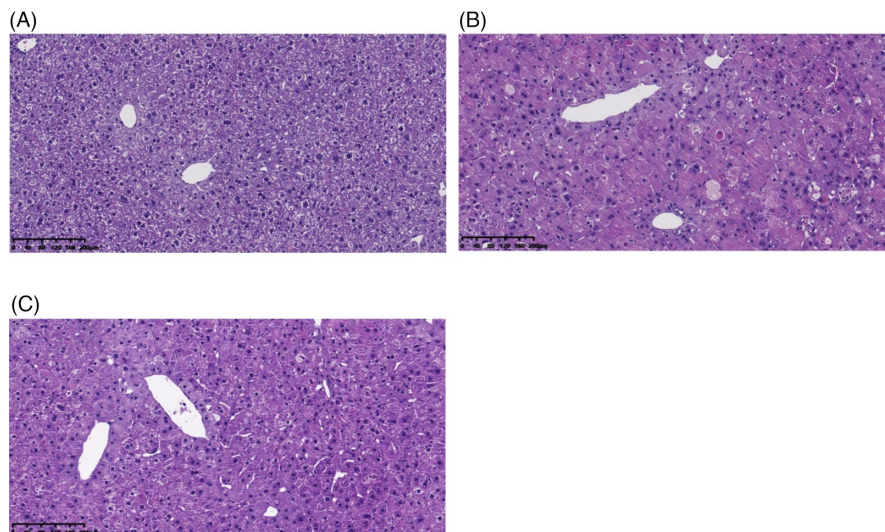


**FIGURE 2** Effects of bicyclol on liver histopathology in HSOS mice by H&E staining. In each group, liver specimens were gathered after 4 weeks of treatment. (A) control group; (B) HSOS group. (C) Bicyclol-pretreated group. Original magnification,  $\times 100$ .

**FIGURE 3** Effects of bicyclol on liver histopathology in HSOS mice by Masson staining. Blue represents collagen while red represents muscle fibers. (A) control group; (B) HSOS group. (C) Bicyclol-pretreated group. (D) Collagen volume fraction % of every group. Original magnification,  $\times 100$ . \* $p < 0.05$  versus control group, # $p < 0.05$  versus HSOS group.

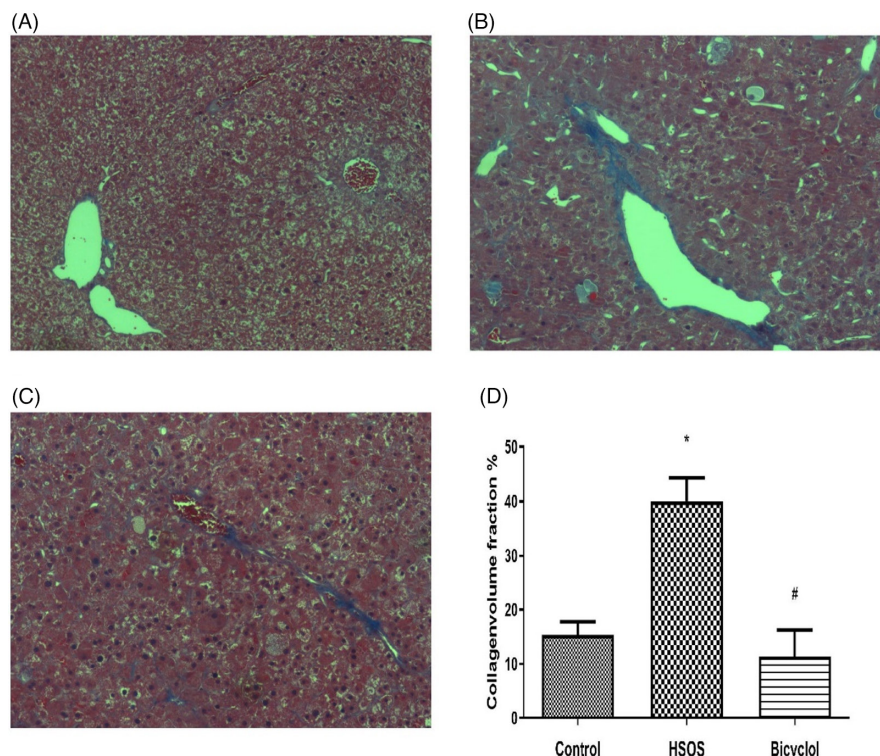


**TABLE 2** H&E staining evaluation of the effect of bicyclol on liver histopathology in *Gynura segetum*-induced HSOS mice.

Parameters	Control group	HSOS model group	Bicyclol group
Central venous endothelial damage and hemorrhage	-	+++	++
Sinusoidal hemorrhage	-	+++	++
Hepatocyte coagulative necrosis	-	+++	++
Fibrosis in portal areas	-	+++	++
Liver lobule structure	normal	Structure disappeared	Presence

Note: "-" represents none of corresponding cells or pathological structures; "+" represents 1-3 of corresponding cells or pathological structures; "++" represents 3-6 of corresponding cells or pathological structures; "+++" represents 7-10 of corresponding cells or pathological structures.

### 3.3 | Effects of bicyclol on mRNA expressions of CYP isozymes in the liver tissues of HSOS mice

As illustrated in Figure 4, the mRNA expression levels of *CYP2b10*, *2c29*, *2c37*, *3a11*, and *7b1* in the HSOS group were obviously declined to 29.8%, 6.2%, 16.9%, 54.8%, and 0.5% compared to the control group, respectively, and the decreasing trend was significantly attenuated by bicyclol pretreatment. Additionally, compared to the control group, *CYP2a5* mRNA expression was upregulated 25-fold in the HSOS group, which was notably downregulated by bicyclol pretreatment.

### 3.4 | Effect of bicyclol on the hepatic apoptosis in HSOS mice

In this study, the TUNEL assay was performed to investigate whether apoptosis is involved in HSOS. As illustrated in

Figure 5, the proportion of apoptotic cells in the liver tissues was higher in the HSOS group than in the control group. Moreover, the proportion was decreased but not significantly by bicyclol pretreatment.

### 3.5 | Effect of bicyclol on the expression levels of caspase-3 and Bcl-2 proteins in the liver tissues of HSOS mice

To further study the function of bicyclol on the hepatocyte apoptosis of HSOS, apoptosis marker proteins, including caspase-3 and Bcl-2, were detected. As illustrated in Figure 6, the protein levels of caspase-3 and Bcl-2 in the liver tissues were notably upregulated in the HSOS group compared to the control group. The upregulation of Bcl-2 was significantly inhibited by bicyclol pretreatment, while it alleviated the upregulation of caspase-3 although not significantly.

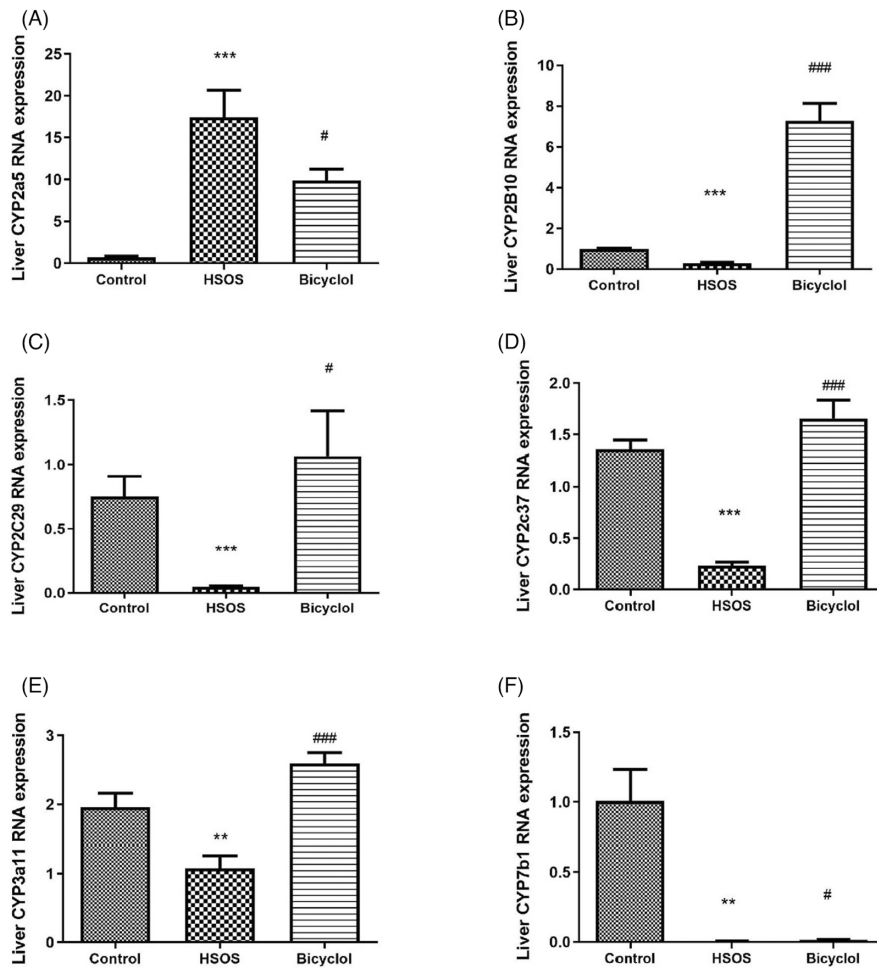


**FIGURE 4** Effects of bicyclol on the mRNA expression of CYP isoforms in HSOS mice. (A) Effect of bicyclol on CYP2a5 mRNA expression in HSOS mice; (B) Effect of bicyclol on CYP2b10 mRNA expression in HSOS mice; (C) Effect of bicyclol on CYP2c29 mRNA expression in HSOS mice; (D) Effect of bicyclol on CYP2c37 mRNA expression in HSOS mice; (E) Effect of bicyclol on CYP3a11 mRNA expression in HSOS mice; (F) Effect of bicyclol on CYP7b1 mRNA expression in HSOS mice. \*\* $p < 0.01$  versus control group, \*\*\* $p < 0.001$  versus control group, # $p < 0.05$  versus HSOS group, ### $p < 0.001$  versus HSOS group.

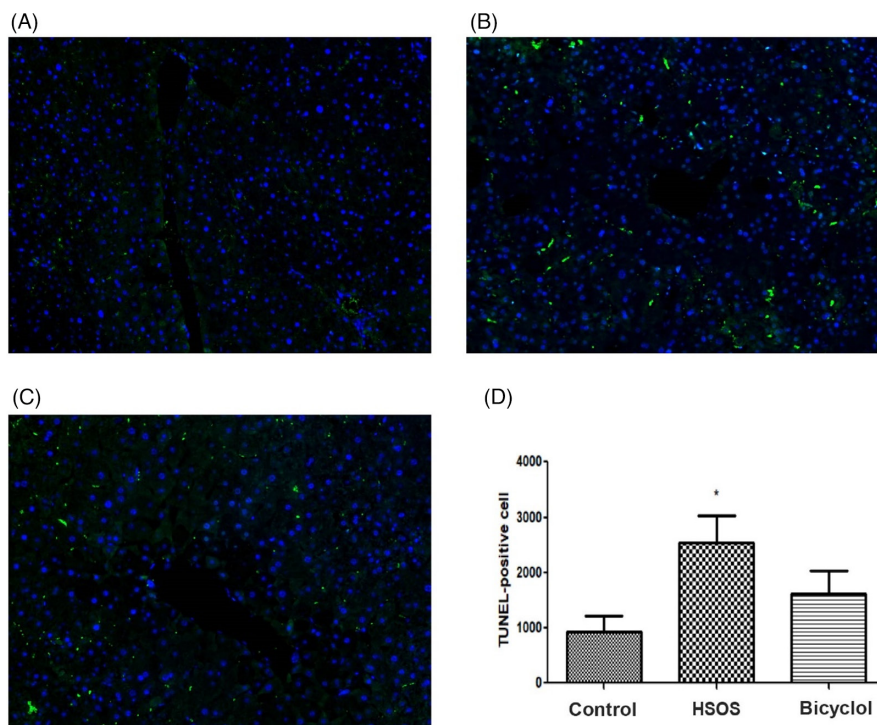


**FIGURE 5** Effect of bicyclol on the increase of hepatic apoptosis in HSOS mice (TUNEL assay). Representative sections of TUNEL staining show apoptosis in mice from the Control, HSOS, and bicyclol-pretreated groups. Foci (green) were quantified using Image J software. (A) Control; (B) HSOS group; (C) Bicyclol-pretreated group; (D) TUNEL-positive cells in every group. Original magnification  $\times 100$ . \* $p < 0.05$  versus control group.

**FIGURE 6** Effect of bicyclol on the protein expression levels of Caspase-3 and Bcl-2 in HSOS mice. Representative immunoblot images of the experiments are shown above, and the graphs below show the corresponding analysis. \* $p < 0.05$  versus control group, \*\*\* $p < 0.001$  versus control group, ## $p < 0.01$  versus HSOS group.

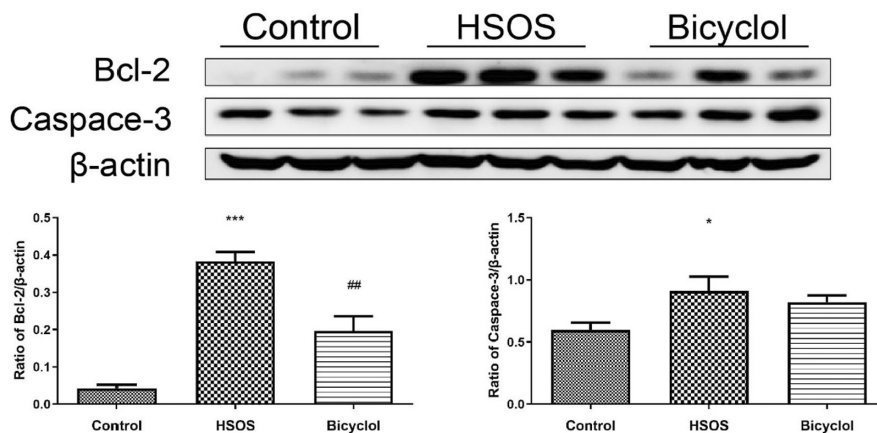
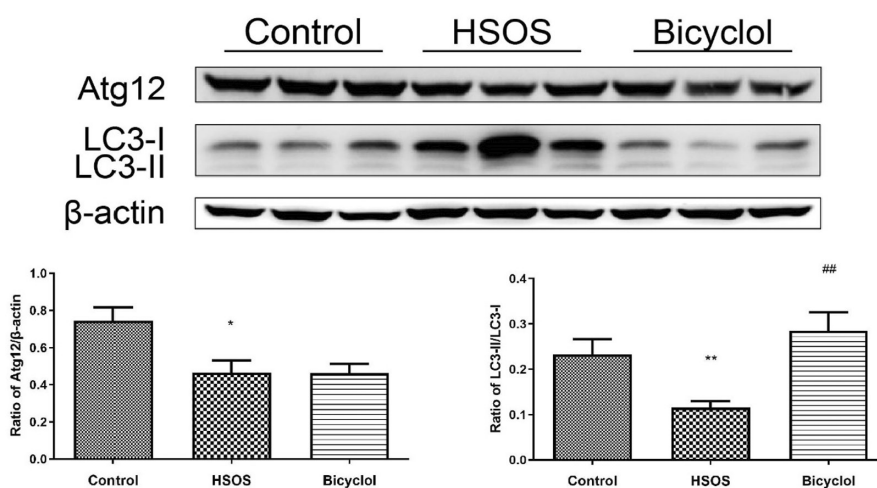


**FIGURE 7** Effect of bicyclol on hepatic autophagy in HSOS mice. Autophagy proteins including LC3 and Atg12 were determined by Western blotting in the liver tissue of every group. Experimentally representative immunoblot images are illustrated above, and the corresponding analysis is shown in the graphs below. \* $p < 0.05$  versus control group, \*\* $p < 0.01$  versus control group, ## $p < 0.01$  versus HSOS group.



### 3.6 | Effect of bicyclol on the hepatic autophagy in HSOS mice

To evaluate the autophagy in *Gynura segetum*-induced HSOS mice, the markers of autophagy, LC3 and Atg12, were detected in the liver tissues. As illustrated in Figure 7, the levels of autophagy-related proteins (LC3-II/LC3-I and Atg12) were downregulated in the HSOS group compared to the control group. Furthermore, bicyclol pretreatment notably inhibited the downregulation of LC3-II/LC3-I in HSOS mice, but it alleviated the downregulation of Atg12, albeit not significantly. Thus, these results showed that bicyclol pretreatment ameliorates the abnormality in CYP450 isoforms.

## 4 | DISCUSSION

The ingestion of *Gynura segetum* was to self-treat trauma, arthritis, pain, and hemorrhage in patients in China, which might lead to the incidence of HSOS despite low-dose consumption (the minimal ingestion was only 10 g).<sup>5</sup> Patients with HSOS induced by *Gynura segetum* may suffer from acute failure and subsequent life-threatening events if they do not receive timely treatment.<sup>17</sup> The results of the

present study revealed that *Gynura segetum* (30 g/kg) administration for 4 weeks induced HSOS in mice, as shown by the increase in serum AST levels, the decrease in serum lipids, and the liver pathological changes, including central venous subendothelial damage and hemorrhage, severe sinusoidal congestion, and fibrosis in some portal areas, which are consistent with previous studies.<sup>14,18</sup> Bicyclol pretreatment (200 mg/kg) exerted an overall protective effect on HSOS induced by *Gynura segetum* in the current study, as evident by inhibiting the elevated serum ALT, raising the levels of serum lipids, and alleviating pathological changes caused by HSOS in mice.

CYP450 isozymes are widely involved in the metabolic activities of endogenous and exogenous substances, such as drugs and environmental compounds.<sup>19</sup> CYP2a5 metabolizes carcinogens, such as nitrosamines and aflatoxin B1, into genotoxic metabolites and is involved in hepatocarcinogenesis, while toxic products of metabolism can induce liver damage.<sup>20</sup> CYP2b10 and CYP3a11 are the markers of two major members of the nuclear receptor superfamily, termed constitutional androstane receptor (CAR) and pregnane X receptor (PXR), respectively,<sup>21</sup> indicating that their levels are representative of the expressions of CAR and PXR. Furthermore, CAR and PXR enhanced the clearance of toxic by-products of endogenous and exogenous chemicals.<sup>22</sup> CYP2c29 and CYP2c37 belong to the CYP2c

subfamily that metabolizes arachidonic acid to bioactive eicosanoids.<sup>23,24</sup> *CYP7b1* mediates several physiological functions, mainly in the liver as bile salt synthesis.<sup>25</sup> In addition, a few drugs and poisons are known to alter the activity of *CYP450* isozymes, such as isoniazid, rifampin, and carbon tetrachloride.<sup>26,27</sup> Some therapeutic drugs can exert therapeutic effects by altering the activity of *CYP450* such as glycyrrhizin.<sup>28</sup> Several previous studies have documented that pyrrolizidine alkaloids are metabolized to dihexyl phthalate esters by hepatic *CYP450* isozymes (*CYP2B* and *CYP3A*) after absorption in the intestine<sup>29–31</sup>; however, whether HSOS induced by *Gynura segetum* poisoning affects the expressions of *CYP450* isozymes is yet to be elucidated. *CYP450* levels might affect various signal transduction pathways that alter the cell cycle, causing apoptosis or aberrant cell growth, and thereby tumorigenesis.<sup>32</sup> Therefore, the mRNA expressions of several *CYP450* isozymes, including *CYP2a5*, *CYP2b10*, *CYP2c29*, *CYP2c37*, *CYP3a11*, and *CYP7b1*, were measured in the present study. The results revealed that *CYP2a5* mRNA expression was notably upregulated in HSOS induced by *Gynura segetum* compared to the control group, while the mRNA expressions of *CYP2b10*, *CYP2c29*, *CYP2c37*, *CYP3a11*, and *CYP7b1* were significantly downregulated. However, bicyclol pretreatment ameliorates the abnormalities of specific *CYP450* isoforms at the mRNA levels during HSOS; the bidirectional regulation might contribute to the hepatoprotective effect. Similarly, Yao et al.<sup>9</sup> reported that bicyclol significantly attenuated the reduction in *CYP2C6*, *CYP3A1/2*, and *CYP2C11* activity and mRNA expression in partial hepatectomy (PH) rat. Bicyclol can upregulate the mRNA and protein expressions of *CYP3A1* and *CYP2E1*. These results showed that bicyclol pretreatment ameliorates abnormality in *CYP450* isoforms during liver regeneration after PH.

Apoptosis is programmed cell death that occurs in a physiological process and in numerous pathological processes.<sup>33</sup> Several drugs or chemicals may cause direct and predictable liver injury, accompanied by hepatocyte apoptosis, which is also involved in *Gynura segetum*.<sup>14,33–37</sup> Consistent results in the current study showed that *Gynura segetum* significantly increases TUNEL-positive cells and upregulates the expression of apoptosis-executing protein Caspase-3 compared to the control. Interestingly, the expression of apoptosis suppressor protein Bcl-2 was dramatically upregulated. Previous studies have shown that bicyclol acts as a hepatoprotective agent by anti-apoptosis in liver injury mice.<sup>38–40</sup> In HepG2 cells intoxicated with D-GalN in vitro, pretreatment with bicyclol remarkably attenuated apoptosis, and the underlying mechanism includes suppression of caspase-3 activity.<sup>41</sup> However, in the present study, an inconspicuous decrease in TUNEL-positive cells and Caspase-3 protein expression after bicyclol pretreatment suggested that apoptosis level was not inhibited. Conversely, apoptosis inhibitory protein Bcl-2 was reduced by bicyclol pretreatment, which could be attributed to the protection of liver damage as the damage was milder than that in the HSOS group. Therefore, bicyclol pretreatment has a potential protective effect owing to the downregulation of inhibitory protein Bcl-2 in HSOS mice.

Autophagy plays a role in maintaining the physiological liver cellular and metabolic homeostasis, while malfunction or dysregulation of autophagy is linked to diverse liver diseases, such as non-alcoholic fatty liver disease, viral hepatitis, drug-induced liver injury, and hepatocellular carcinoma.<sup>42,43</sup> Consequently, a novel therapeutic approach for targeting autophagy is emerging for liver diseases.<sup>44</sup> Our previous study recently reported that autophagy was impaired in response to *Gynura segetum*-induced HSOS in mice.<sup>14</sup> The finding was further extended by the present results showing that the levels of Atg12 and LC3-II/LC3-I proteins were markedly downregulated in HSOS mice, while that of Bcl-2, a blocker of autophagy occurrence, was dramatically upregulated.<sup>45</sup> Bicyclol pretreatment substantially reversed the altered protein expressions of both LC3-II/LC3-I and Bcl-2, while that of Atg12 was less pronounced. These results suggested that bicyclol contributes to the hepatoprotective effect in HSOS mice via recovery of autophagy. Compared to other hepatoprotective and anticoagulant drugs, bicyclol can exert both hepatoprotective and enzyme-lowering effects and also improve the abnormalities of *CYP450* induced by *Gynura segetum* and alleviate the downregulation of autophagy of hepatocytes, thereby providing a new strategy therapeutic for HSOS.

## 5 | CONCLUSION

In conclusion, the present study demonstrated that bicyclol effectively attenuated HSOS induced by *Gynura segetum*, which could be attributed to the regulated expressions of *CYP450* isozymes and alleviated the downregulation of autophagy.

As bicyclol exerts these anti-HSOS effects, it may be further assessed for the treatment of HSOS induced by *Gynura segetum*.

## AUTHOR CONTRIBUTIONS

Design of the study: LH, YXM, and YJZ; Preparation of Figures and Tables, Interpretation of the data and Writing the original draft: YJZ, WJY, and JS; Technical procedures: YJZ, WJY, JS, SJP, ZX, and XZP; Performing statistical analysis: ZH and ZX; Revision and modification of the manuscript: LH and YXM.

## ACKNOWLEDGMENTS

This work was supported by Ningbo Digestive System Tumor Clinical Medicine Research Center (2019A21003), Project of Zhejiang Medical and Health Platform Plan (2022KY1079), Zhejiang Provincial Medicine and Health Technology Project (2020RC106), Ningbo Science and Technology Program Public Welfare Project (2019C50066, 2021S098, 2021S144), Ningbo Public Welfare Science & Technology Major Project (2021S106), Ningbo Natural Science Foundation Project (202003N4336) and Zhejiang Provincial Public Technology Research Projects (LGF22H310003).



## CONFLICT OF INTEREST

The authors declare no conflict of interest.

## DATA AVAILABILITY STATEMENT

The data that support the findings of this study are available from the corresponding author upon reasonable request.

## ORCID

Jingping Shao  <https://orcid.org/0000-0001-8642-4194>

Zeping Xu  <https://orcid.org/0000-0002-5703-4194>

Xiaomin Yao  <https://orcid.org/0000-0002-0806-846X>

## REFERENCES

- DeLeve LD, Valla DC, Garcia-Tsao G. Vascular disorders of the liver. *Hepatology*. 2009;49(5):1729-1764.
- Plessier A, Rautou PE, Valla DC. Management of hepatic vascular diseases. *J Hepatol*. 2012;56(Suppl 1):S25-S38.
- Wang JY, Gao H. Tusanqi and hepatic sinusoidal obstruction syndrome. *J dig Dis*. 2014;15(3):105-107.
- Tang J, Hattori M. pyrrolizidine alkaloids-containing Chinese medicines in the Chinese pharmacopoeia and related safety concerns. *Yao Xue Xue Bao*. 2011;46(7):762-772.
- Cooperative Group for Health and Gall Diseases. Chinese Society of Gastroenterology, Chinese Medical Association. Expert consensus on diagnosis and treatment of pyrrolizidine alkaloids-related sinusoidal obstruction syndrome (2017, Nanjing). *J Clin Hepatol*. 2017;33:1627-1637.
- Yang XQ, Ye J, Li X, Li Q, Song YH. Pyrrolizidine alkaloids-induced hepatic sinusoidal obstruction syndrome: pathogenesis, clinical manifestations, diagnosis, treatment, and outcomes. *World J Gastroenterol*. 2019;25(28):3753-3763.
- Liu GT. Bicyclol: a novel drug for treating chronic viral hepatitis B and C. *Med Chem*. 2009;5(1):29-43.
- Zhao TM, Wang Y, Deng Y, et al. Bicyclol attenuates acute liver injury by activating autophagy, anti-oxidative and anti-inflammatory capabilities in mice. *Front Pharmacol*. 2020;11:463.
- Yao XM, Wang BL, Gu Y, Li Y. Effects of bicyclol on the activity and expression of CYP450 enzymes of rats after partial hepatectomy. *Yao xue xue bao*. 2011;46(6):656-663.
- Yao XM, Zhao J, Li Y, Li Y. Effects of bicyclol on liver regeneration after partial hepatectomy in rats. *Dig Dis Sci*. 2009;54(4):774-781.
- Yu HY, Wang BL, Zhao J, Yao XM, Gu Y, Li Y. Protective effect of bicyclol on tetracycline-induced fatty liver in mice. *Toxicology*. 2009;261(3):112-118.
- Zhao J, Chen H, Li Y. Protective effect of bicyclol on acute alcohol-induced liver injury in mice. *Eur J Pharmacol*. 2008;586(1-3):322-331.
- Yao X, Li H, Chen L, Zhu N, Zhang X, Cheng X. Effects of Bicyclol on the expression of cytochrome P450 after liver injury induced by isoniazid and rifampicin in mice. *J Biomater Tissu Eng*. 2018;8(8):1209-1215.
- Zhang H, Jia S, Jin L, et al. *Gynura segetum* induces hepatic sinusoidal obstruction syndrome in mice by impairing autophagy. *Acta Cir Bras*. 2022;36(11):e361104.
- Zhu H, Chu Y, Huo J, Chen Z, Yang L. Effect of prednisone on transforming growth factor- $\beta$ 1, connective tissue growth factor, nuclear factor- $\kappa$ Bp65 and tumor necrosis factor- $\alpha$  expression in a murine model of hepatic sinusoidal obstruction syndrome induced by *Gynura segetum*. *Hepatal Res*. 2011;41(8):795-803.
- DeLeve LD, McCuskey RS, Wang X, et al. Characterization of a reproducible rat model of hepatic veno-occlusive disease. *Hepatology*. 1999;29(6):1779-1791.
- Zhang Z, Zou H, Dai Z, et al. *Gynura segetum*-induced liver injury leading to acute liver failure: a case report and literature review. *BMC Complement Med Ther*. 2022;22(1):61.
- Yu XZ, Ji T, Bai XL, et al. Expression of MMP-9 in hepatic sinusoidal obstruction syndrome induced by *Gynura segetum*. *J Zhejiang Univ Sci B*. 2013;14(1):68-75.
- Zhang L, Xu X, Badawy S, et al. A review: effects of macrolides on CYP450 enzymes. *Curr Drug Metab*. 2020;21(12):928-937.
- Abu-Bakar A, Hakkola J, Juvonen R, Rahnasto-Rilla M, Raunio H, Lang MA. Function and regulation of the Cyp2a5/CYP2A6 genes in response to toxic insults in the liver. *Curr Drug Metab*. 2013;14(1):137-150.
- Wang Z, Wu Q, Li X, Klaunig JE. Constitutive androstane receptor (CAR) mediates dieldrin-induced liver tumorigenesis in mouse. *Arch Toxicol*. 2020;94(8):2873-2884.
- Timsit YE, Negishi M. CAR and PXR: the xenobiotic-sensing receptors. *Steroids*. 2007;72(3):231-246.
- Graves JP, Gruzdev A, Bradbury JA, DeGraff LM, Edin ML, Zeldin DC. Characterization of the tissue distribution of the mouse Cyp2c subfamily by quantitative PCR analysis. *Drug Metab Dispos*. 2017;45(7):807-816.
- Luo G, Zeldin DC, Blaisdell JA, Hodgson E, Goldstein JA. Cloning and expression of murine CYP2Cs and their ability to metabolize arachidonic acid. *Arch Biochem Biophys*. 1998;357(1):45-57.
- Stiles AR, McDonald JG, Bauman DR, Russell DW. CYP7B1: one cytochrome P450, two human genetic diseases, and multiple physiological functions. *J Biol Chem*. 2009;284(42):28485-28489.
- Madan A, Graham RA, Carroll KM, et al. Effects of prototypical microsomal enzyme inducers on cytochrome P450 expression in cultured human hepatocytes. *Drug Metab Dispos*. 2003;31(4):421-431.
- Zhang X, Kuang G, Wan J, et al. Salidroside protects mice against CCl4-induced acute liver injury via down-regulating CYP2E1 expression and inhibiting NLRP3 inflammasome activation. *Int Immunopharmacol*. 2020;85:106662.
- Sun H, Wang J, Lv J. Effects of glycyrrhizin on the pharmacokinetics of paeoniflorin in rats and its potential mechanism. *Pharm Biol*. 2019;57(1):550-554.
- Lu Y, Wong KY, Tan C, Ma J, Feng B, Lin G. Establishment of a novel CYP3A4-transduced human hepatic sinusoidal endothelial cell model and its application in screening hepatotoxicity of pyrrolizidine alkaloids. *J Environ Sci Health C Toxicol Carcinog*. 2020;38(2):169-185.
- Ma J, Xia Q, Fu PP, Lin G. Pyrrole-protein adducts - a biomarker of pyrrolizidine alkaloid-induced hepatotoxicity. *J Food Drug Anal*. 2018;26(3):965-972.
- Huan JY, Miranda CL, Buhler DR, Cheeke PR. The roles of CYP3A and CYP2B isoforms in hepatic bioactivation and detoxification of the pyrrolizidine alkaloid senecionine in sheep and hamsters. *Toxicol Appl Pharmacol*. 1998;151(2):229-235.
- Nebert DW, Dalton TP. The role of cytochrome P450 enzymes in endogenous signalling pathways and environmental carcinogenesis. *Nat Rev Cancer*. 2006;6(12):947-960.
- Iorga A, Dara L. Cell death in drug-induced liver injury. *Adv Pharmacol*. 2019;85:31-74.
- Iorga A, Dara L, Kaplowitz N. Drug-induced liver injury: cascade of events leading to cell death, apoptosis or necrosis. *Int J Mol Sci*. 2017;18(5):1018.
- Wang W, Yang X, Chen Y, et al. Seneciphylline, a main pyrrolizidine alkaloid in *Gynura japonica*, induces hepatotoxicity in mice and primary hepatocytes via activating mitochondria-mediated apoptosis. *J Appl Toxicol*. 2020;40(11):1534-1544.
- Li DP, Chen YL, Jiang HY, et al. Phosphocreatine attenuates *Gynura segetum*-induced hepatocyte apoptosis via a SIRT3-SOD2-mitochondrial reactive oxygen species pathway. *Drug Des Devel Ther*. 2019;13:2081-2096.

37. Jia S, Chen Q, Wu J, et al. Danshensu derivative ADTM ameliorates CCl<sub>4</sub>induced acute liver injury in mice through inhibiting oxidative stress and apoptosis. *Pathol Res Pract*. 2021;228:153656.
38. Yao XM, Li Y, Li HW, Cheng XY, Lin AB, Qu JG. Bicyclol attenuates tetracycline-induced fatty liver associated with inhibition of hepatic ER stress and apoptosis in mice. *Can J Physiol Pharmacol*. 2016;94(1):1-8.
39. Bao XQ, Liu GT. Induction of overexpression of the 27- and 70-kDa heat shock proteins by bicyclol attenuates concanavalin A-induced liver injury through suppression of nuclear factor-kappaB in mice. *Mol Pharmacol*. 2009;75(5):1180-1188.
40. Bao XQ, Liu GT. Bicyclol: a novel antihepatitis drug with hepatic heat shock protein 27/70-inducing activity and cytoprotective effects in mice. *Cell Stress Chaperones*. 2008;13(3):347-355.
41. Li M, Liu GT. Inhibition of Fas/FasL mRNA expression and TNF-alpha release in concanavalin A-induced liver injury in mice by bicyclol. *World J Gastroenterol*. 2004;10:1775-1779.
42. Qian H, Chao X, Williams J, et al. Autophagy in liver diseases: a review. *Mol Aspects Med*. 2021;82:100973.
43. Williams JA, Ding WX. Role of autophagy in alcohol and drug-induced liver injury. *Food Chem Toxicol*. 2020;136:111075.
44. Ueno T, Komatsu M. Autophagy in the liver: functions in health and disease. *Nat Rev Gastroenterol Hepatol*. 2017;14(3):170-184.
45. Wang K. Autophagy and apoptosis in liver injury. *Cell Cycle*. 2015;14(11):1631-1642.

**How to cite this article:** Yao J, Wu J, Jia S, et al. Effects of bicyclol on hepatic sinusoidal obstruction syndrome induced by *Gynura segetum*. *J Clin Lab Anal*. 2022;36:e24793. doi:[10.1002/jcla.24793](https://doi.org/10.1002/jcla.24793)